



---

## Numerical Analysis of Statical Shear Behaviour of Reinforced Concrete Haunched Beams Strengthened by Using Externally Bounded Steel Plates by ANSYS Program

Abd El-Rahman Megahid Ahmed<sup>1</sup>, Omar A. Farghal<sup>1</sup>, Ahmed Mohamed Sayed<sup>1,2</sup>, Omar Ali Yassen<sup>3</sup>

<sup>1</sup>Civil Engineering dept. Faculty of Engineering, Assuit University, Assuit, Egypt

<sup>2</sup>On Leave to Majmaah University, Majmaah, Kingdom of Saudi Arabia

<sup>3</sup>Civil Engineering in (SCWW) Company, Sohag, Egypt

---

**Abstract** This paper present the nonlinear finite element analysis (FEA) that has been carried out to simulate the behavior of failure modes of reinforced concrete (RC) beams strengthened in shear by external bounded steel plates. The search consisted of fifty two but this paper presents four beams were modeled in FEM software using ANSYS. In those four beams, one beam is without steel plates and three beams strengthened by steel plates with different width of steel plates. From the analyses the load-deflection relationships, crack pattern, first crack load and ultimate load was obtained and compared with the experimental results available in literature. The load-deflection plots obtained from numerical studies show good agreement with the experimental plots. There was a difference in behavior between the RC beams strengthened with and without steel plates. Therefore, modeling of experimental beams can be adoptable in ANSYS. Validation of experimental results can also be done using ANSYS.

**Keywords** Haunched Beams, ANSYS Program, finite element analysis (FEA), reinforced concrete (RC)

---

### Introduction

Strengthening of concrete haunched beams with bonded external steel plates in shear is becoming on increasing by popular retrofit technique among researchers and engineering worldwide. Concrete of higher compressive strength have been produced currently and increasing used by the designers and contractors. The use of finite element analysis has increased due to progressing knowledge and capabilities of computer software and hardware. It has now become the choice method to analysis concrete structural components. The use of computer software to model these elements is much faster and extremely cost-effective. The goal of this research is study attempts to compare the results from elastic analysis of R.C beams under transverse loading by using an analysis software to that obtained from a normal experimental study in lab.

The shear behavior of reinforced concrete haunched beams has been investigated experimentally by many researchers [1-6]. The matching between the experimentally work and theoretically work has been reached to more than 95%.

Nonlinear finite element analysis (FEA) of reinforced concrete beams have been performed by many researchers [7-11] studied shear behaviour of reinforced concrete beams by using finite element analysis (ANSYS).

### Beam Geometry

The model is 150 cm total length with rectangular cross-section of 12 cm breadth and constant height equals to 28 cm. along the mid zone of beam 40cm and variable height along the shear span of beams equals to 36cm. these beams were tests under equal loads of 40 cm apart. All beams were reinforced with four tension bars from high tensile steel of 16.0 mm diameter and two compression bars of 10.0 mm diameter plus stirrups of 6.0 mm



diameter at variable spacing as shown in Fig.1 and Fig.2. The external steel plates were different width in a variable depth, as shown in Fig.3.

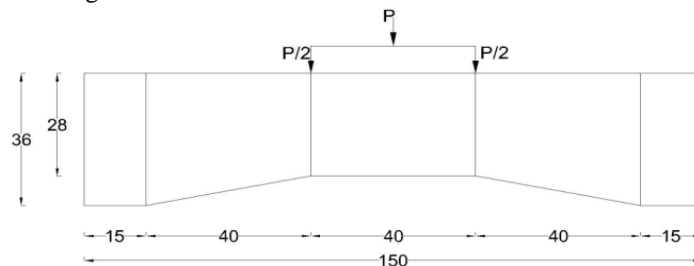


Figure 1: Details of loading and dimensions

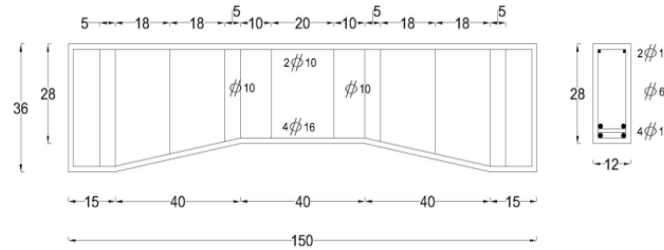


Figure 2: Details of reinforcement of tested beams

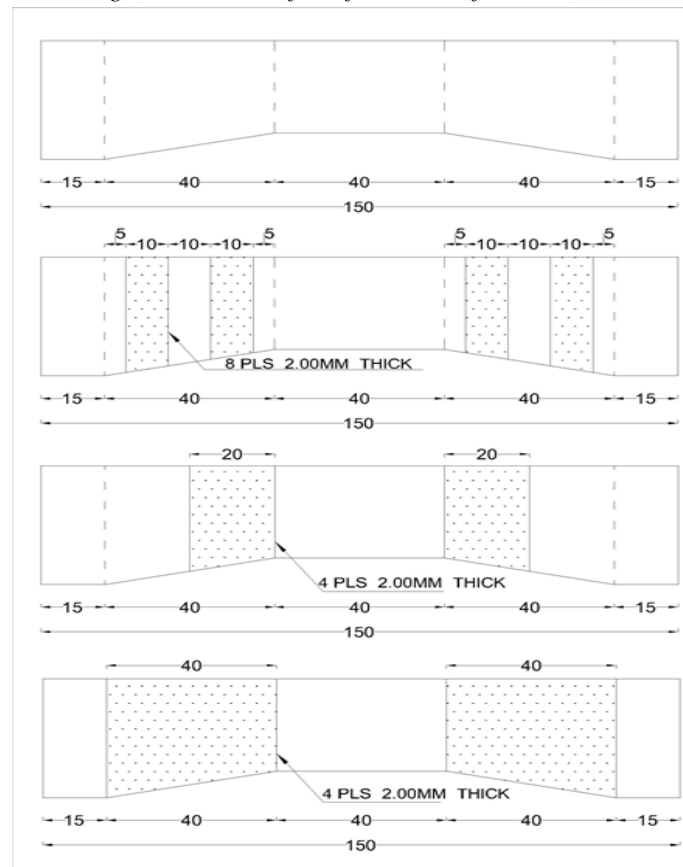


Figure 3: Arrangement of bonded steel plates

### Analytical Investigation

Advances in field of computer-aided engineering during the last two decades have been quite extensive and have led to considerable benefits to many engineering industries. In the building industry, use of advanced finite element tools not only allowed the introduction of innovative and efficient building products, but also the development of accurate design methods. Here SOLID65, LINK8 and SOLID186 elements are used to model RC beams.



**Concrete Modeling**

The solid 65 element was used to model the concrete. This element has eight nodes ,with three degrees of freedom at each node and translations in the nodal x- ,y-and z- directions. This element is capable of plastic deformation ,cracking in three orthogonal directions and crushing. The geometry and the nodes of this element are shown in Fig.4.

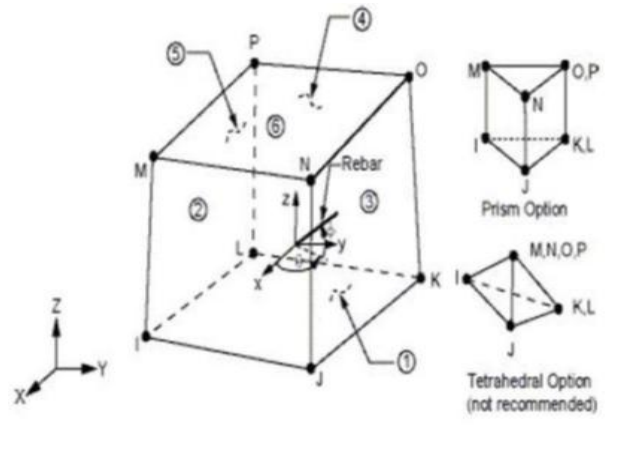


Figure 4: Solid 65 element (ANSYS)

**Steel Reinforcement Modeling**

A Link 8 element was used to model the steel reinforcement. This element is a 3D spar element with two nodes and three degrees of freedom at each node x- ,y-and z- directions. This element is also capable of plastic deformation. The geometry and node locations for this element type are shown in Fig.5.

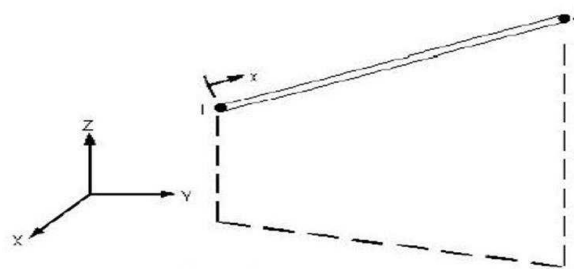


Figure 5: Link 8 element (ANSYS)

**Steel Plates Modeling**

A Solid 186 element was used for the steel plates at the supports for the beam. This element has eight nodes , with three degrees of freedom at each node translations in the x- ,y-and z- directions. The geometry and the nodes of this element are shown in Fig.6.

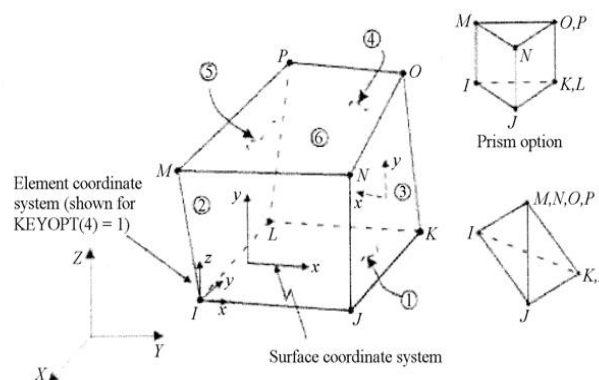


Figure 6: Solid 186 element (ANSYS)

### Meshing Model

A finite element analysis requires meshing of the model. In other words, the model is divided into a number of small elements. The bond strength between the concrete and steel reinforcement should be considered. To provide the perfect bond, the link element for the steel reinforcing was connected between nodes of each adjacent concrete solid element, so the two materials shared the same nodes. The same approach was adopted for steel plates. The maximum element has dimension 2.00mm \* 2.00mm \* 2.00mm. Meshing beams are shown in Fig 7.

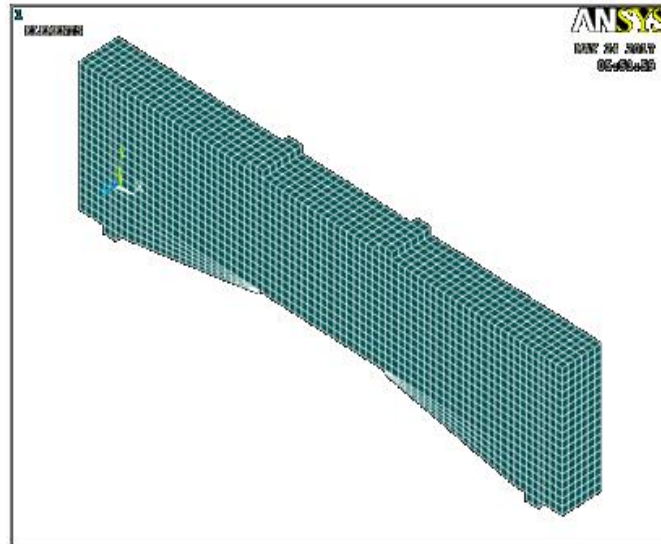
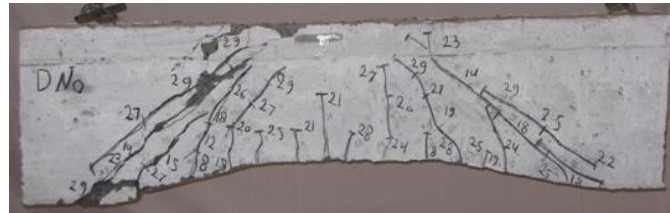


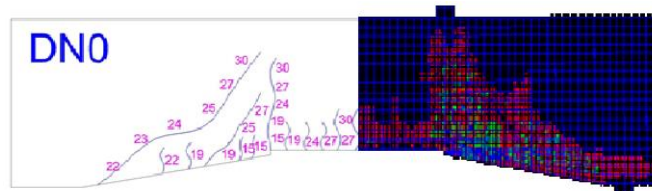
Figure 7: Meshing for control beam

### Pattern of Cracks and Modes of Failure

The first crack for original beam "DN.0" is observed at bottom concrete surface at one third of shear span (towards point of haunch end) or from small depth and by increasing applied load it increases the crack at shear zone and small cracks were observed at tension zone in concrete cover. The final mode of failure was of shear type one in haunch zone with inclination of (45°) with vertical axis, as shown in Fig.8.



(a) Experimental.



(a) Theoretical.

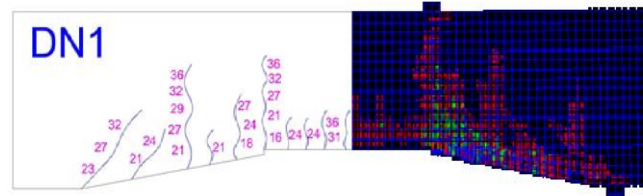
Figure 8: Crack pattern of beam "DN.0"(a) Experimental & (b) Theoretical

The first crack for strengthened beam "DN.1" started vertically at bottom concrete surface in constant depth under point of load application. By increasing applied load the major crack formed at shear zone. The mode of failure was of shear compression type the crack failure is observed starting from bottom concrete surface between the strengthened plates at haunch zone, as shown in Fig.9.





(a) Experimental.



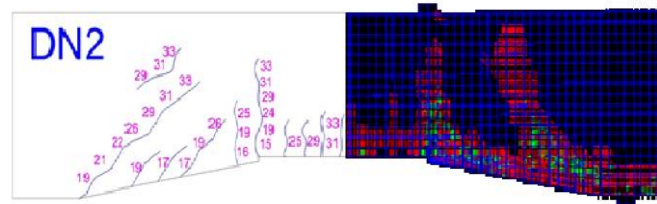
(b) Theoretical.

Figure 9: Crack pattern of beam "DN.1" (a) Experimental & (b) Theoretical.

The first crack for strengthened beam "DN.2" started vertically at bottom concrete surface in constant depth under point of load application. By increasing applied load the major crack formed at shear zone. The mode of failure was of shear compression type the crack failure is observed starting from bottom concrete surface from beginning the haunch, as shown in Fig.10.



(a) Experimental.



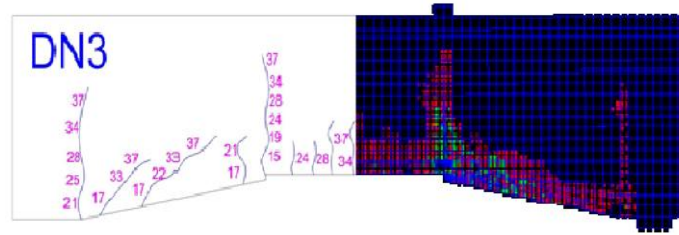
(b) Theoretical.

Figure 10: Crack pattern of beam "DN.2" (a) Experimental & (b) Theoretical

The first crack for strengthened beam "DN.3" started vertically at bottom concrete surface in constant depth under point of load application. By increasing applied load the major crack formed at flexure zone. The mode of failure was of flexure type one the crack failure is observed starting from bottom concrete surface from beginning the haunch and at mid span at compression zone, as shown in Fig.11.



(a) Experimental.



(b) Theoretical.

Figure 11: Crack pattern of beam "DN.3" (a) Experimental & (b) Theoretical

**The Matching and Results for Beams**

**Load-Deflection Curves**

At the position of maximum deflection the measured values at the bottom surface are plotted against the applied load from zero loading up to failure for all different tested beams. All measured and plotted values indicated that the deflection increases as the applied load increases. The relation between the applied load and corresponding maximum deflection is approximately linear at the beginning of the relation up to nearly the cracking load and mostly nonlinear relation at higher load levels. The inclination of such linear relation mainly is depending upon various parameters included in this study.

For series "DN" (cube strength = 700 kg/cm<sup>2</sup>), Fig.12, the rate of decreasing is considered small for beams "DN.2" but it is considerably big for beam "DN.1" and "DN.3". The difference between these rates for beams "DN.1" and "DN.3" is considerably big.

Also the measured maximum load and deflection at failure point for strengthened beams "DN.3", "DN.1" and "DN.2" is considered very big for that of the original beam "DN.0". In deflection at failure point the difference between these rates for beams "DN.1" and "DN.2" is considerably big and it is considerably big for beams "DN.3".

The matched between the theoretical work and experimental work, it is prove that the extent of accuracy of finite element analysis (FEA) that achieves the same laboratory results and the match ratio of up to 95% of the results of the laboratory.

To clarify the theoretical work and practical work correspondence between the relationship between the ultimate load and deflection.as shown in Fig.13 to Fig.16.

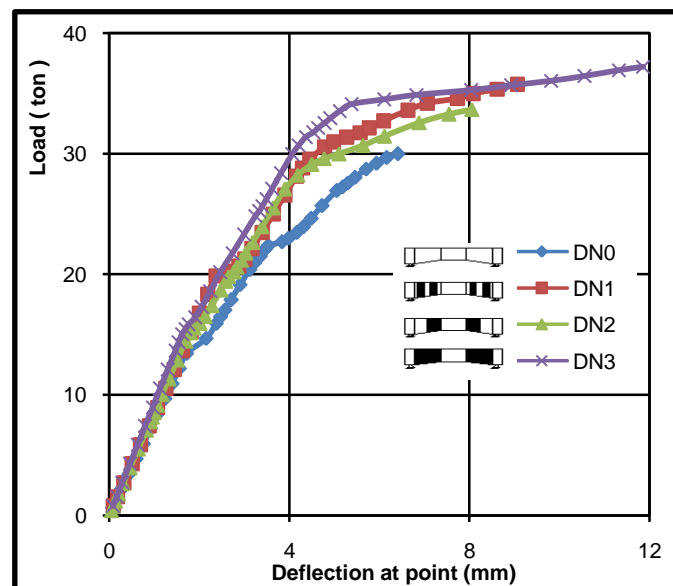


Figure 12: Load deflection curves for beams "DN.0", "DN.1", "DN.2" and "DN.3" of series ( $F_{CU} = 700 \text{ kg/cm}^2$ )

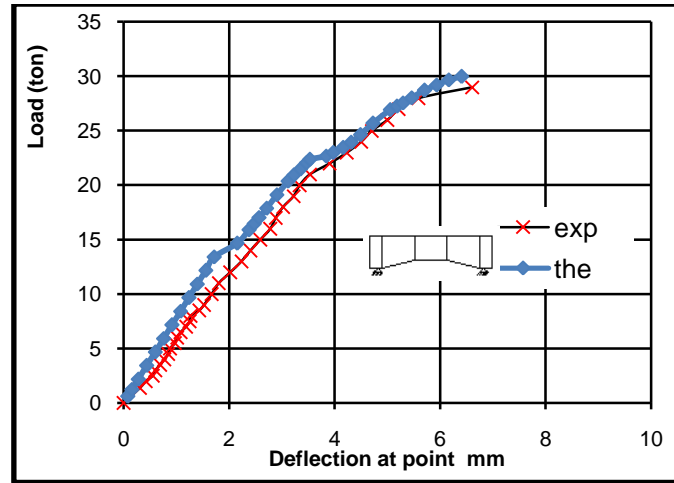


Figure 13: Load deflection curves for beam "DN.0" theoretical and experimental of series ( $F_{CU} = 700 \text{ kg/cm}^2$ ).

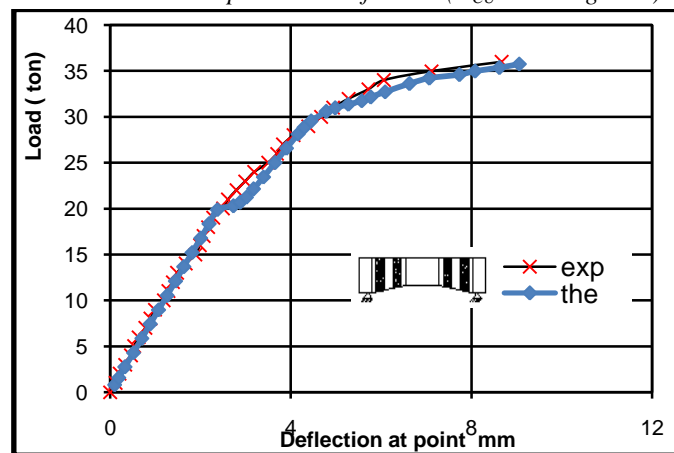


Figure 14: Load deflection curves for beam "DN.1" theoretical and experimental of series ( $F_{CU} = 700 \text{ kg/cm}^2$ ).

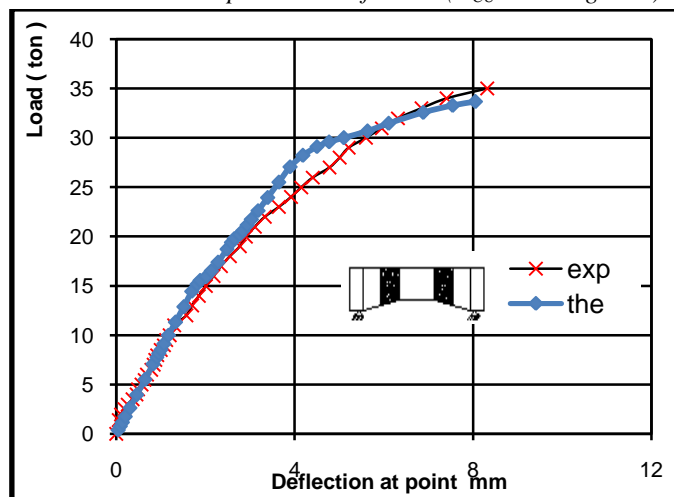


Figure 15: Load deflection curves for beam "DN.2" theoretical and experimental of series ( $F_{CU} = 700 \text{ kg/cm}^2$ ).

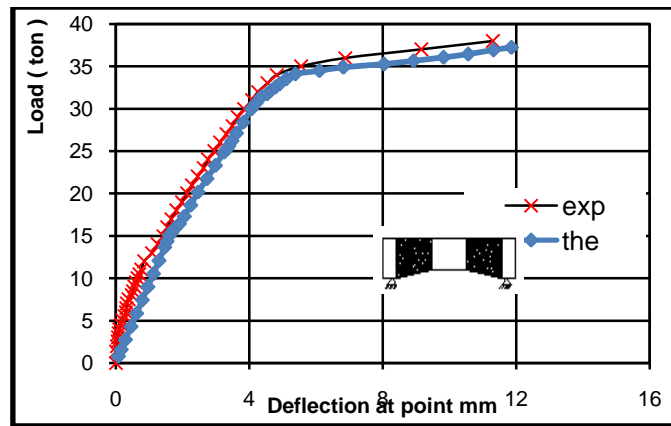


Figure 16: Load deflection curves for beam "DN.3" theoretical and experimental of series ( $F_{CU} = 700 \text{ kg/cm}^2$ ).

**Load-Compression Concrete Strain Curves**

For series "DN" ( $F_{cu} = 700 \text{ kg/cm}^2$ ), Fig.17, the rate of decreasing is considered big for beams "DN.1" and "DN.2" but it is considerably very big for beam "DN.3". The difference between these rates for beams "DN.1" and "DN.2" is considerably small. Also the measured maximum concrete strain at failure point for strengthened beam "DN.3" is considered very big to be crushing of concrete zone for that of the beam "DN.0", "DN.1" and "DN.2".

To clarify the theoretical work and practical work correspondence between the relationship between the ultimate load and compression concrete strain, as shown in Fig.18 to Fig.21.

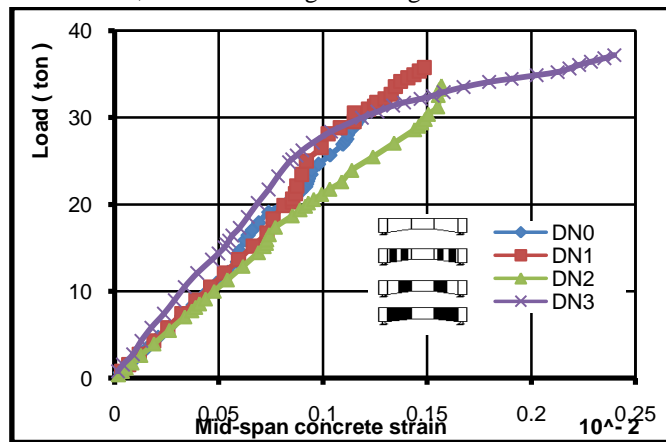


Figure 17: Load- concrete strain in compression face curves for beams "DN.0", "DN.1", "DN.2" and "DN.3" from series ( $F_{CU} = 700 \text{ kg/cm}^2$ )

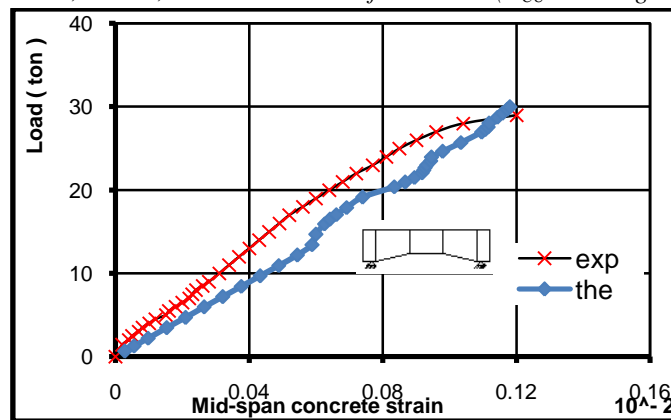


Figure 18: Load-concrete strain curves for obtained theoretical and experimental beam (DN0) for series ( $F_{CU} = 700 \text{ kg/cm}^2$ ).

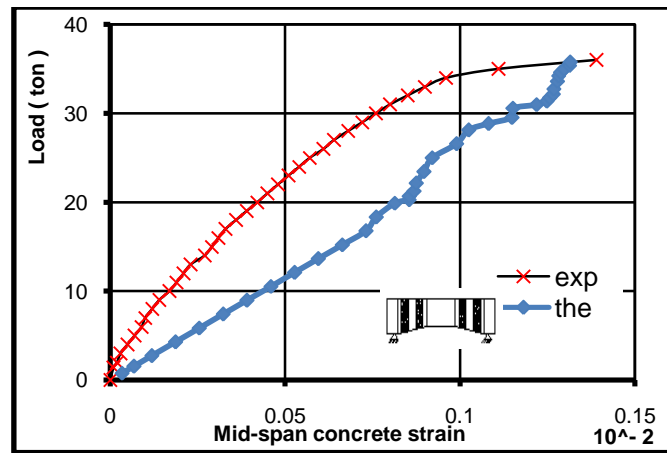


Figure 19: Load-concrete strain curves for obtained theoretical and experimental beam (DN1) for series ( $F_{cu} = 700 \text{ kg/cm}^2$ ).

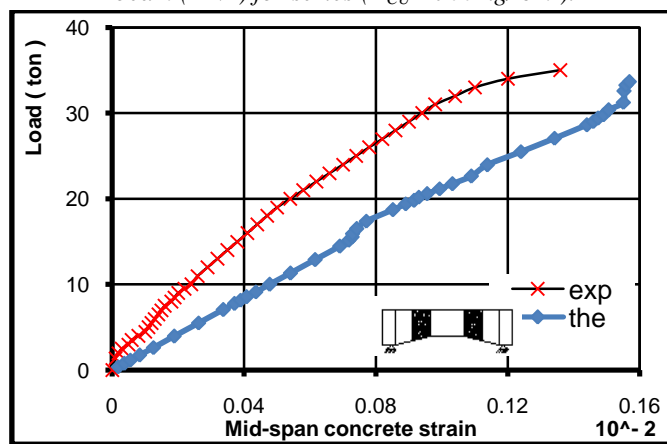


Figure 20: Load-concrete strain curves for obtained theoretical and experimental beam (DN2) for series ( $F_{cu} = 700 \text{ kg/cm}^2$ ).

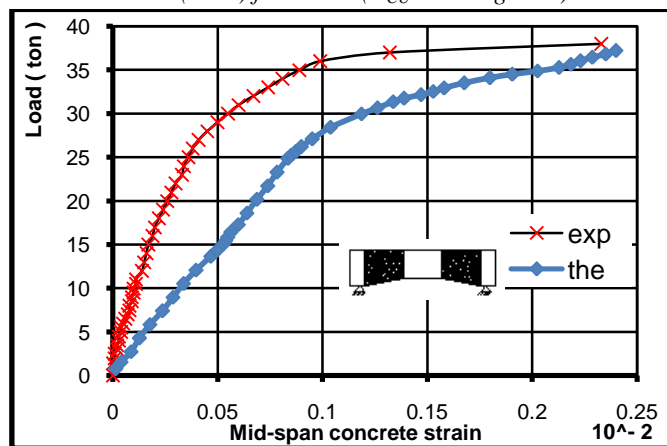


Figure 21: Load-concrete strain curves for obtained theoretical and experimental beam (DN3) for series ( $F_{cu} = 700 \text{ kg/cm}^2$ ).

**Load-Tension Steel Strain Curves.**

At mid-span point, steel strain is measured of maximum values at the bottom surface are plotted against the applied load from zero loading up to failure for the different tested beams.

series "DN" ( $F_{cu} = 700 \text{ kg/cm}^2$ ), Fig.22, the rate of decreasing is considered big for beams "DN.1" and "DN.2" but it is considerably very big for beam "DN.3". The difference between these rates for beams "DN.1" and

"DN.2" is considerably small. Also the measured maximum steel strain at failure point for strengthened beam "DN.3" is considered very big to be crushing of concrete zone for that of the beam "DN.0", "DN.1" and "DN.2". To clarify the theoretical work and practical work correspondence between the relationship between the ultimate load and tension steel strain. as shown in Fig.23 to Fig.26.

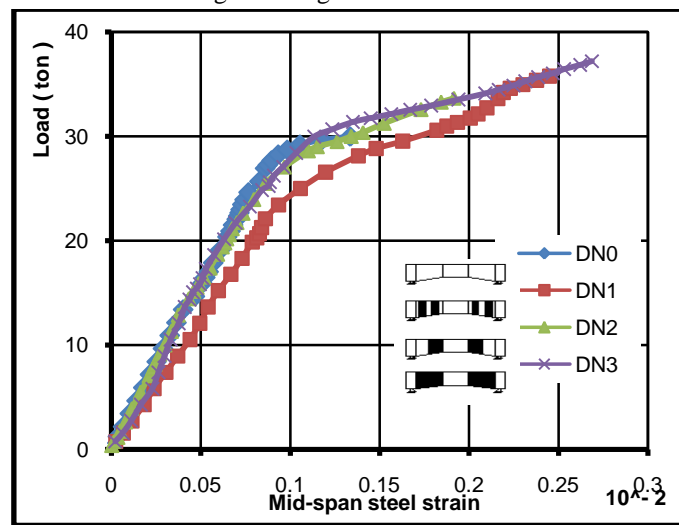


Figure 22: Load- steel strain curves for beams "DN.0", "DN.1", "DN.2" and "DN.3" from series ( $F_{cu} = 700 \text{ kg/cm}^2$ ).

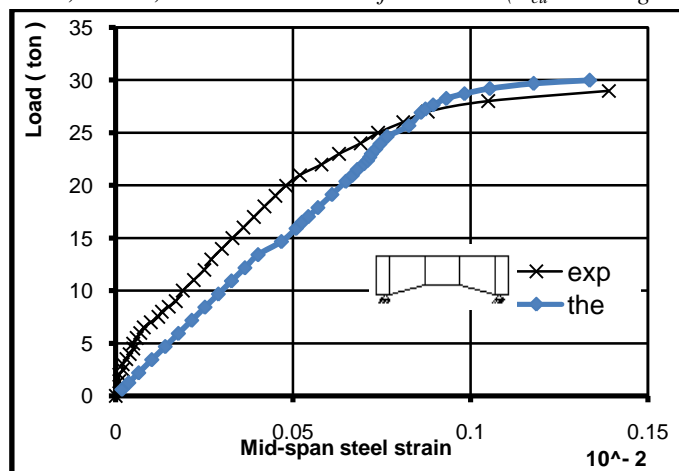


Figure 23: Load -steel strain curves for obtained theoretical and experimental beam "DN.0" from series ( $F_{cu} = 700 \text{ kg/cm}^2$ ).

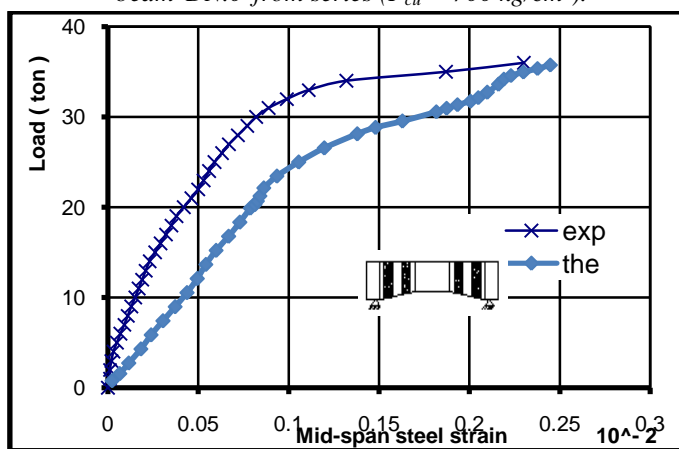


Figure 24: Load -steel strain curves for obtained theoretical and experimental beam "DN.1" from series ( $F_{cu} = 700 \text{ kg/cm}^2$ ).

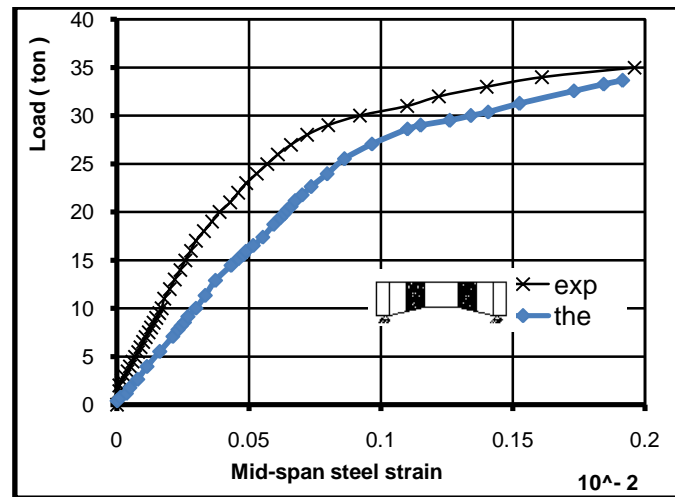


Figure 25: Load -steel strain curves for obtained theoretical and experimental beam "DN.2" from series ( $F_{cu} = 700 \text{ kg/cm}^2$ ).

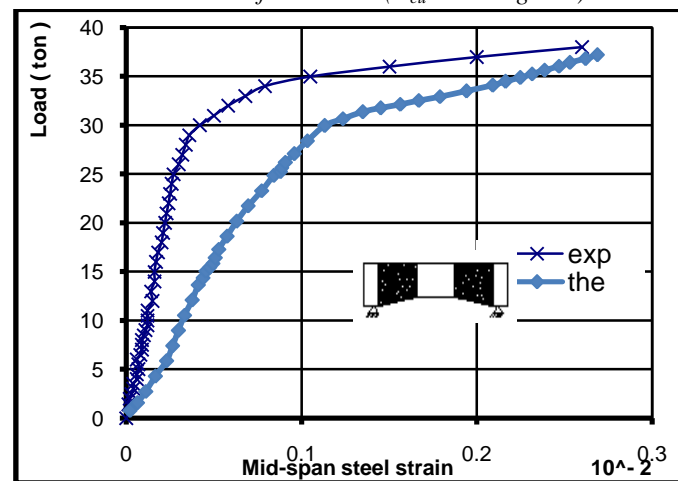


Figure 26: Load -steel strain curves for obtained theoretically and experimental beam "DN.3" from series ( $F_{cu} = 700 \text{ kg/cm}^2$ ).

### Discussion and Analysis of obtained Results

#### Effect of Width, Arrangement and Position of Bonded Side Steel Plates:

For strengthened beams "DN.1", "DN.2" and "DN.3" having negative haunch ( $\tan\alpha=0.2$ ) it was observed that, by increasing the ratio of area of strengthened plate to area of haunched original beam and change the position of plates, the cracking load was changed to 1.11, 1.03 and 1.05 times than of the original beam "DN.0" for case of beams having area of steel side plate to area of haunched original beam of about 0.50, 0.469 and 1.00 respectively, as shown in Fig.27. But the ultimate load was increased to 1.19, 1.12 and 1.24 times than of the original beam "DN.0" respectively, as shown in Fig.27.

From Fig.12, for all grades concrete it was obvious that for beams having negative haunch, in general, by increasing the applied load the maximum deflection increases for all beams. The rate of increasing is mainly depend on the ratio of area of strengthened plates to area of haunched original beam and the position of the side plates on haunched. The maximum measured value of deflection at failure point for strengthened beams is bigger than the original beams, as shown in Fig.28.

From Fig.17 and Fig.22, for all grades concrete it was obvious that for beams having negative haunch ( $\tan\alpha=0.2$ ), in general, the effect of ratio of area of strengthened plates to area of haunched original beam and the position of bonded side plates on concrete compression strain and steel tension strain are the same as that on maximum deflection, as shown in Fig.29. Also the measured maximum mid-span concrete strain and steel tension strain at failure point for strengthened beams "DN.3" is considered very big to be crushing of concrete at



compression zone for that of the beams “DN.0”, “DN.1” and “DN.2”. The matching between theoretical work and experimental work had shown in Table 1 and 2.

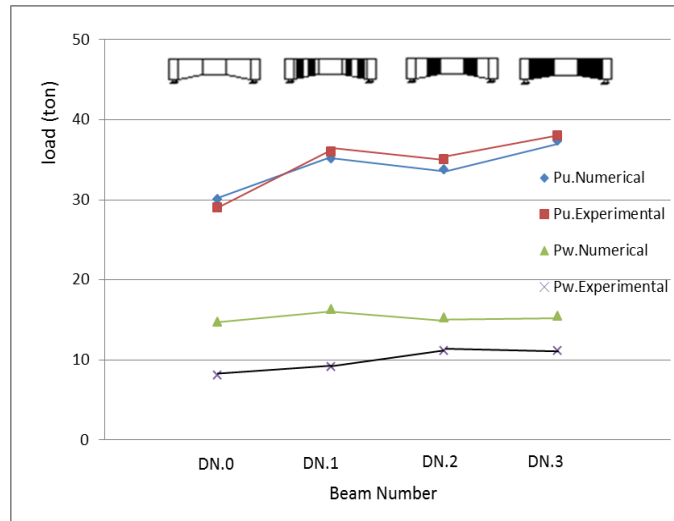


Figure 27: Relation between ultimate, working load and configuration of external bonded steel plates for experimental and numerical beams ( $F_{cu} = 700\text{kg/cm}^2$ )

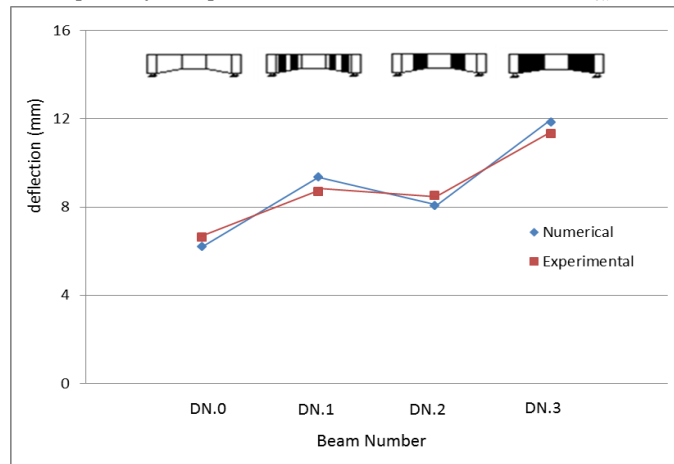


Figure 28: Relation between the deflection and configuration of external bonded steel plates for experimental and numerical beams ( $F_{cu} = 700\text{kg/cm}^2$ )

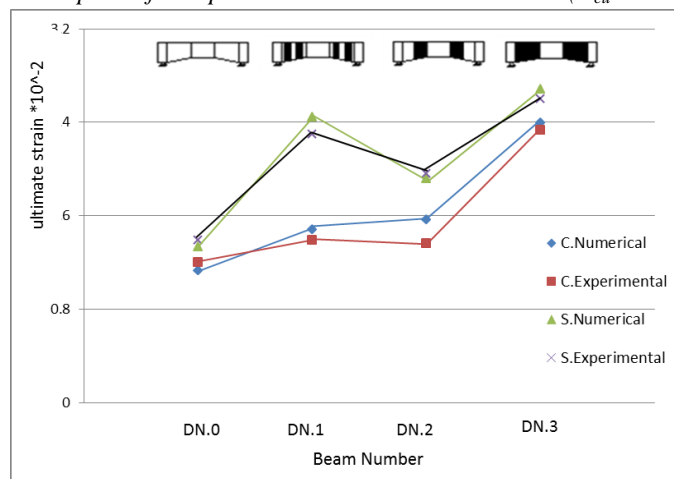


Figure 29: Relation between the compression concrete, tension steel strain and configuration of external bonded steel plates for experimental and numerical beams ( $F_{cu} = 700\text{kg/cm}^2$ )

**Table 1:** The compression between the experimental and numerical studies for beams

Beam No.	Ultimate load			Deflection		
	Experimental	Numerical	Matching ratio	Experimental	Numerical	Matching ratio
DN.0	29	29.98	0.96	6.61	6.69	0.98
DN.1	36	35.76	0.99	8.67	9.36	0.92
DN.2	35	33.66	0.96	8.32	8.15	0.97
DN.3	38	37.23	0.97	11.3	11.85	0.95

**Table 2:** The compression between the experimental and numerical studies for compression concrete and tension steel strain

Beam No.	Compression Concrete Strain			Tension Steel Strain		
	Experimental	Numerical	Matching ratio	Experimental	Numerical	Matching ratio
DN.0	120	118.0	0.983	139	133.6	0.96
DN.1	139	148.5	0.935	230	244.7	0.93
DN.2	136	156.8	0.866	196	191.5	0.97
DN.3	233	239.92	0.971	260	268.6	0.967

### Conclusions

The numerical analysis of statically shear behavior of reinforced concrete beams by using (ANSYS Program) based on nonlinear finite element analysis (FEA) has been successful and the numerical results have shown a good correlation with experimental results. The following conclusions results of the research:

- Increasing the strength of concrete, the number of cracks decreases at the same level of loading, and both of cracking and ultimate loads increase. But the mode of failure is the same for strengthened and unstrengthened beams for all grades of concrete.
- Increasing the grade of concrete, the maximum deflection, mid-span concrete and steel reinforced bars strain decrease at any loading level before failure level. However at the final failure level the maximum deflection, mid-span concrete and steel reinforcement bars strain increase by increasing the grade of concrete.
- Generally, the effectiveness of strengthening increases by increasing the area of strengthened steel side plates, its position on haunch and its thickness, but decreases relatively by increasing the grade of concrete strength.

### References

- [1]. ACI Committee 503 Proposed Standard 503.1: Standard Specification for Bonded Hardened Concrete, Steel, Wood, Brick and Another Materials to Hardened Concrete with a Multi-Component Epoxy Adhesive “,ACI Journal, Sept. 1978, pp.437 .
- [2]. Omar A. F. Ahmed, Static Behaviour of Reinforced Concrete Beams Strengthened by Using Epoxy Bonded External Steel Plates , Assiut University. Egypt, 1993.
- [3]. Omar A. F. Ahmed, Shear Strengthening of R.C Beams Using Carbon Fiber Reinforced Polymer (CFRP) Sheets , International Conference on Structural and Geotechnical Engineering and Construction Technology , El-Mansoura University , Egypt , March 2004
- [4]. Ahmed Mohamed Sayed, Static Behaviour of Reinforced High Strength Concrete Haunched Beams Strengthened by Using Epoxy Bonded External Steel Plates, Assiut University. Egypt, 2010.
- [5]. Debaiky S.Y. and EL-Niema, E.I. “Behaviour and Strength of R.C. Haunched Beams in Shear”, ACI Journal, 1982.
- [6]. Abd EL-magid M.A. “Repeated loading Effect on the Behaviour of Haunched R.C. Beams” M.SC. Thesis, Assiut University, 1982.
- [7]. Ahmed Mohamed Sayed, Modeling Advancement for Beams Strengthened with FRP Composites, Southeast University, Nanjing, China, 2014.



- [8]. R. Srinivasan and K. Sathiya, Flexural Behavior of Reinforced Concrete Beams Using Finite Element Analysis ,Tehnica University , Gheorghe, 2010.
- [9]. Alfeehan A.A., “Strengthening Of R.C. Beams By External Steel Plate Using Mechanical Connection Technique”; Journal of Engineering and Development, 2014.
- [10]. Musmar M. A., Rjoub M. I. and Abdel Hadi M. A. “Nonlinear Finite Element Analysis of Shallow Reinforced Concrete Beams using SOLID65 Element”; ARPJ Journal of Engineering and Applied Sciences, 2014.
- [11]. Mohamed R. Abdulkadir, Zana A.Aziz and Jaza H. Muhammad. “Nonlinear Finite Element Analysis of Reinforced Concrete Beams Strengthened with Externally Bonded Steel Plate using ANSYS” Sulaimani Journal for Engineering Sciences, 2017.

